

s.d. = 0.000014; E&A ($n = 8$), mean ($2\sigma_m$) = 0.708008(13), s.d. = 0.000020. A polynomial least-squares fit to NBS-987 variance during the analysis period was used to drift-compensate measured ratios relative to a baseline of 0.710242. Compensations for these samples ranged from -0.000015 to 0.000009.

Received 4 December 2002; accepted 17 March 2003; doi:10.1038/nature01575.

1. Carpenter, S. J., Erickson, J. M., Lohmann, K. C. & Owen, M. R. Diagenesis of fossiliferous concretions from the Upper Cretaceous Fox Hills Formation, North Dakota. *J. Sedim. Petrol.* **58**, 706–723 (1988).
2. McArthur, J. M., Kennedy, W. J., Chen, M., Thirlwall, M. F. & Gale, A. S. Strontium isotope stratigraphy for Late Cretaceous time: direct numerical calibration of the Sr isotope curve based on the US Western Interior. *Palaeogeogr. Palaeoclimatol. Palaeoecol.* **108**, 95–119 (1994).
3. Barrera, E. & Savin, S. in *Evolution of the Cretaceous Ocean–Climate System* (eds Barrera, E. & Johnson, C. C.) 245–282 (Geol. Soc. Am. Spec. Pap. 332, 1999).
4. Wilf, P., Johnson, K. R. & Huber, B. T. Correlated terrestrial and marine evidence for global climate changes before the mass extinction at the Cretaceous–Paleogene boundary. *Proc. Natl Acad. Sci. USA* **100**, 599–604 (2003).
5. Frizzell, D. L. Otoliths of new fish (*Vorhisia vulpes*, N. Gen., N. Sp. Siluroidei?) from Upper Cretaceous of South Dakota. *Copeia* **2**, 178–181 (1965).
6. Wolfe, J. A. & Upchurch, G. R. Jr North American nonmarine climates and vegetation during the Late Cretaceous. *Palaeogeogr. Palaeoclimatol. Palaeoecol.* **61**, 33–77 (1987).
7. Barron, E. J., Fawcett, P. J., Pollard, D. & Thompson, S. Model simulations of Cretaceous climates: the role of geography and carbon dioxide. *Phil. Trans. R. Soc. Lond. B* **341**, 307–315 (1993).
8. Patterson, W. P., Smith, G. R. & Lohmann, K. C. in *Continental Climate Change from Isotopic Indicators* (eds Swart, P., Lohmann, K. C., McKenzie, J. & Savin, S.) 191–202 (Am. Geophys. Un. Monogr., 1993).
9. Thorrold, S. R., Campana, S. E., Jones, C. M. & Swart, P. K. Factors determining $\delta^{13}\text{C}$ and $\delta^{18}\text{O}$ fractionation in aragonitic otoliths of marine fish. *Geochim. Cosmochim. Acta* **61**, 2909–2919 (1997).
10. Wurster, C. M. & Patterson, W. P. Late Holocene climate change for the eastern interior United States: evidence from high-resolution $\delta^{18}\text{O}$ values of sagittal otoliths. *Palaeogeogr. Palaeoclimatol. Palaeoecol.* **170**, 81–100 (2001).
11. Ivany, L. C., Patterson, W. P. & Lohmann, K. C. Increase in seasonality across the Eocene–Oligocene boundary inferred from high-resolution microsampling of fossil otoliths, US Gulf Coastal Plain. *Nature* **407**, 887–890 (2000).
12. Andrus, C. F. T., Crowe, D. E., Sandweiss, D. H., Reitz, E. J. & Romanek, C. S. Otolith $\delta^{18}\text{O}$ record of Mid-Holocene sea surface temperatures in Peru. *Science* **295**, 1508–1511 (2002).
13. Patterson, W. P. Oldest isotopically characterized fish otoliths provide insight to Jurassic continental climate of Europe. *Geology* **27**, 199–202 (1999).
14. Waage, K. M. *The Type Fox Hills Formation, Cretaceous (Maestrichtian), South Dakota*, Part 1. *Stratigraphy and Palaeoenvironments* (Peabody Museum of Natural History, Yale University, Bulletin 27, 1968).
15. Erickson, J. M. in *Proc. F. D. Holland, Jr., Geol. Symp.* (eds Erickson, J. M. & Hoganson, J. W.) 199–241 (North Dakota Geological Survey Miscellaneous Series no. 76, 1992).
16. Erickson, J. M. The Dakota Isthmus—closing the Late Cretaceous Western Interior Seaway. *North Dakota Acad. Sci. Proc.* **53**, 124–129 (1999).
17. Carpenter, S. J., Erickson, J. M. & Hoganson, J. W. Isotopic characterization of the Late Cretaceous Fox Hills – Hell Creek Estuary of North and South Dakota. *Geol. Soc. Am. Abstr. Program* 31–32 (2002).
18. Nolf, D. & Stringer, G. L. in *Mesozoic Fishes: Systematics and Paleocology*, Proc. Int. Meeting (eds Arratia, G. & Vieh, G.) 433–459 (Friedrich Pfeil, München, 1996).
19. Shackleton, N. J. & Kennett, J. P. Paleotemperature history of the Cenozoic and initiation of Antarctic glaciation: Oxygen and carbon isotope analyses in Deep Sea Drilling Project Sites 277, 279, and 281. *Init. Rep. DSDP* **74**, 761–776 (1975).
20. Randall, R. G., Healy, M. C. & Dempson, J. B. in *Common Strategies of Anadromous and Catadromous Fishes* (eds Dadswell, M. J. et al.) 27–41 (American Fisheries Society, Bethesda, Maryland, 1987).
21. Healy, M. C. & Groot, C. in *Common Strategies of Anadromous and Catadromous Fishes* (eds Dadswell, M. J. et al.) 298–312 (American Fisheries Society, Bethesda, Maryland, 1987).
22. Peterson, B. J. & Fry, B. Stable isotopes in ecosystem studies. *Annu. Rev. Ecol. Syst.* **18**, 293–320 (1987).
23. Schwarcz, H. P. et al. Stable carbon isotope variations in otoliths of Atlantic cod (*Gadus morhua*). *Can. J. Aquat. Sci.* **55**, 1798–1806 (1998).
24. Weidman, C. R. & Millner, R. High-resolution stable isotope records from North Atlantic cod. *Fisheries Res.* **46**, 327–342 (2000).
25. Wurster, C. M. & Patterson, W. P. Metabolic rate of late Holocene freshwater fish: evidence from $\delta^{13}\text{C}$ values of otoliths. *Paleobiology* (in the press).
26. McCormick, S. D. & Saunders, R. L. in *Common Strategies of Anadromous and Catadromous Fishes* (eds Dadswell, M. J. et al.) 211–229 (American Fisheries Society, Bethesda, Maryland, 1987).
27. Ursin, E. in *Symp. Zool. Soc. Lond.* **44**, 63–87 (1979).
28. Huddleston, R. W. & Savoie, K. M. Teleostean otoliths from the Late Cretaceous (Maestrichtian age) Severn Formation of Maryland. *Proc. Biol. Soc. Wash.* **96**, 658–663 (1983).
29. Dettman, D. L. & Lohmann, K. C. Oxygen isotope evidence for high-altitude snow in the Laramide Rocky Mountains of North America during the Late Cretaceous and Paleogene. *Geology* **28**, 243–246 (2000).

Supplementary Information accompanies the paper on www.nature.com/nature.

Acknowledgements We thank G. Ludvigson, L. Gonzalez, T. White, H. Schwarcz and W. Patterson for comments on preliminary drafts of the manuscript, and N. Miller for strontium isotope analyses of biogenic carbonates.

Competing interests statement The authors declare that they have no competing financial interests.

Correspondence and requests for materials should be addressed to S.J.C. (scott-j-carpenter@uiowa.edu).

Fitness costs of R-gene-mediated resistance in *Arabidopsis thaliana*

D. Tian*, M. B. Traw*, J. Q. Chen†, M. Kreitman* & J. Bergelson*

* Department of Ecology and Evolution, University of Chicago, 1101 E. 57th Street, Chicago, Illinois 60637, USA

† Department of Biology, Nanjing University, 22 Han Kou Road, Nanjing 210093, People's Republic of China

Resistance genes (R-genes) act as an immune system in plants by recognizing pathogens and inducing defensive pathways. Many R-gene loci are present in plant genomes, presumably reflecting the need to maintain a large repertoire of resistance alleles. These loci also often segregate for resistance and susceptibility alleles that natural selection has maintained as polymorphisms within a species for millions of years^{1–5}. Given the obvious advantage to an individual of being disease resistant, what prevents these resistance alleles from being driven to fixation by natural selection? A cost of resistance⁶ is one potential explanation; most models require a lower fitness of resistant individuals in the absence of pathogens for long-term persistence of susceptibility alleles⁷. Here we test for the presence of a cost of resistance at the *RPM1* locus of *Arabidopsis thaliana*. Results of a field experiment comparing the fitness of isogenic strains that differ in the presence or absence of *RPM1* and its natural promoter reveal a large cost of *RPM1*, providing the first evidence that costs contribute to the maintenance of an ancient R-gene polymorphism.

RPM1 codes for a peripheral plasma membrane protein⁸ that confers the ability to recognize *Pseudomonas syringae* pathogens carrying *AvrRpm1* or *AvrB*^{9,10}. Susceptible individuals lack the entire coding region of *RPM1* (ref. 10), so there is a single susceptible allele at this locus. Both resistance and susceptibility alleles frequently occur together within natural populations and are common across the range of *A. thaliana*³. Molecular evolutionary analysis of the non-coding DNA flanking *RPM1* indicates that the resistance and susceptibility alleles have coexisted for more than nine million years³. The great age of this polymorphism indicates that the susceptibility allele might be maintained by natural selection due to a cost of resistance, because other mechanisms of coexistence can be eliminated. First, heterozygote advantage can be excluded by *A. thaliana*'s high selfing rate¹¹. Second, there is no evidence of geographic differentiation between allelic classes³. Last, because the susceptibility allele is deleted for the entire locus¹⁰, it cannot have differential adaptive values in alternative environments.

To test for a fitness cost of *RPM1* expression, we inserted a 3.84-kilobase (kb) region from Columbia containing *RPM1*, its promoter and its full terminator¹⁰ into a susceptible ecotype, Bla-2, to create four independent transgenic lines. Transgenic plants containing this fragment have been shown to respond to infection with pathogenic *P. syringae* DC3000:AvrRpm1 by eliciting the appropriate hypersensitive response (D. Boyes and J. L. Dangl, personal communication). The *RPM1* gene fragment was placed between two *lox* sites¹². To induce recombinational excision of the *RPM1* transgene, we crossed each replicate line with a Bla-2 line expressing *cre* recombinase and created selfed lines that had lost the *RPM1* transgene. This allowed us to generate independent pairs of homozygous lines with identical genetic backgrounds differing only with respect to the presence or absence of the *RPM1* gene. Individuals within each pair shared a common insertion site for the introduced DNA, but resistant individuals (*RPM1*⁺) expressed *RPM1* and the selectable marker, kanamycin, whereas susceptible individuals (*RPM1*⁻) expressed only kanamycin. The creation of paired lines effectively controls for fitness changes caused by the

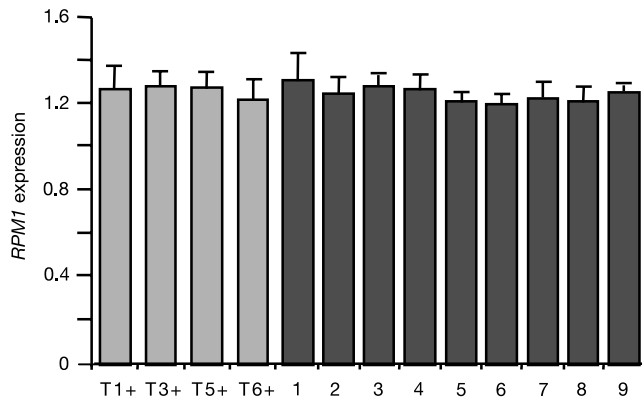


Figure 1 *RPM1* expression. Normalized expression levels (*RPM1* threshold cycle (C_T) divided by endogenous C_T) in *RPM1*⁺ transgenic plants (light grey bars) and nine accessions that possess *RPM1* naturally (dark grey bars; 1, Bur-0; 2, Col-0; 3, Ct-0; 4, Kas-1; 5, Lip-0; 6, Pog-0; 7, Tsu-0; 8, Tamm-7; 9, Wu-0). No *RPM1* expression was detected in the susceptible Bla-2 ecotype or the four *RPM1*⁻ transgenic lines. Results are means \pm s.e.m.

introduction of the foreign DNA (and a selectable marker) into each location in the genome.

We confirmed the appropriateness of our paired transgenic lines for use in fitness trials in six ways. First, we sequenced the transgenic *RPM1* alleles to confirm that they were unchanged. Second, we used anchor PCR¹³ to determine that each transgene landed in a non-coding DNA location with no known function. Third, we used direct sequencing to confirm that excisions occurred precisely at the *lox* sites, thus removing only the *RPM1* locus. Fourth, we verified that the *RPM1*⁺, but not *RPM1*⁻, lines elicited a hypersensitive response after treatment with *P. syringae* DC3000 carrying *AvrRpm1* (ref. 14). Fifth, we used quantitative real-time PCR to show that background (that is, uninduced) levels of *RPM1* expression in our transgenic lines were indistinguishable from expression levels of ecotypes carrying the *RPM1* allele (Fig. 1). Last, to further confirm that our transgenic lines did not overexpress *RPM1*, we tested for induction of the salicylic acid pathway. Our measurement of endogenous free salicylic acid and a defence induced by the salicylate-dependent pathway (peroxidase activity) failed to reveal any differences between the *RPM1*⁺ and *RPM1*⁻ lines (Table 1). Furthermore, growth of *P. syringae* pv. *tomato* DC3000 did not differ between *RPM1*⁺ and *RPM1*⁻ lines (Table 1). These results

indicate ‘normal’ functioning of the *RPM1* transgene in our experimental lines.

In late spring 2001, we transplanted 500 replicates of each line into the field, and grew them to maturity in the absence of detectable disease. To monitor for pathogenic bacteria, we collected and cultured bacteria from representatives of each plant line twice during plant growth. Although numerous bacterial isolates were collected, we found that they were not pathogenic and did not carry *AvrRpm1* or *AvrB*. When plants senesced, we counted the number of siliques per plant and the number of seeds per silique, and measured the dry biomass of each shoot. *RPM1*⁺ plants tended to have fewer siliques and seeds per silique, as well as lower shoot biomass than the paired *RPM1*⁻ plants (Table 2). More importantly, we found that *RPM1*⁺ individuals suffered, on average, a 9% decrease in total seed production relative to their *RPM1*⁻ counterparts (Fig. 2). There was no significant variation among the four pairs of transgenic lines in the magnitude of this cost of resistance (one-way analysis of variance on difference in total seed production between paired plants: $F_{3,1257} = 0.48$, $P > 0.6$). This consistency across independent transformed lines indicates that fitness loss was not a consequence of ectopic *RPM1* expression caused by position effects.

Given the large magnitude of this fitness cost, we asked whether the cost of resistance might have been an unintended consequence of inserting *RPM1* into a susceptible genetic background containing inappropriate alleles for an interacting cofactor. One such cofactor is *RIN4*, a gene that physically interacts with *RPM1* and is necessary for elicitation of a hypersensitive response¹⁵. Although *RIN4* and *RPM1* are not genetically linked, we hypothesized that, with strong epistasis, there might be permanent linkage disequilibrium between the two loci. We determined the *RPM1* genotype and the *RIN4* gene sequences of 96 ecotypes; no evidence for association between alleles at these two loci could be detected (Table 3). Indeed, Bla-2 contains a haplotype (type 3) of *RIN4* that is more commonly found in resistant individuals. Thus, we find no evidence for a mismatch between *RPM1* and *RIN4* alleles that could explain the fitness cost, but this does not rule out the possibility that other, as yet unidentified, cofactors are involved.

Two features of our experimental system facilitated the ability to detect a pleiotropic cost of *RPM1* resistance. First, we used genetic engineering to remove potentially confounding effects of linkage. Second, the susceptible allele, because it is a deletion of the entire locus, completely eliminates any possible direct or indirect cost of producing and expressing a ‘susceptible’ protein variant. Indeed, it has been suggested¹⁶ that previous failures to detect costs of R-gene resistance stemmed from a misclassification of ‘defeated’ (but

Table 1 Effect of *RPM1* presence or absence on the salicylate-dependent pathway

Line	Salicylic acid concentration (mmol per g dry leaf)			Peroxidase activity ($A_{470} \text{ min}^{-1}$ per mg total protein)			Bacterial growth (log colony-forming units)		
	<i>RPM1</i> ⁺	<i>RPM1</i> ⁻	<i>P</i>	<i>RPM1</i> ⁺	<i>RPM1</i> ⁻	<i>P</i>	<i>RPM1</i> ⁺	<i>RPM1</i> ⁻	<i>P</i>
T1	0.011 \pm 0.001	0.011 \pm 0.001	0.939	34.2 \pm 20.0	34.3 \pm 25.4	0.996	8.0 \pm 0.3	7.6 \pm 0.1	0.292
T3	0.012 \pm 0.002	0.013 \pm 0.001	0.674	7.7 \pm 3.3	4.6 \pm 1.0	0.887	7.5 \pm 0.2	7.6 \pm 0.1	0.832
T5	0.011 \pm 0.001	0.009 \pm 0.001	0.767	24.3 \pm 9.5	28.8 \pm 11.8	0.844	8.1 \pm 0.4	7.8 \pm 0.1	0.386
T6	0.012 \pm 0.001	0.016 \pm 0.006	0.412	44.4 \pm 24.8	24.4 \pm 11.6	0.388	7.9 \pm 0.3	7.4 \pm 0.6	0.211

Results are means \pm s.e.m.

Table 2 Effect of *RPM1* presence or absence on correlates of fitness

Line	No. of siliques per plant			No. of seeds per silique			Shoot dry biomass (g)		
	<i>RPM1</i> ⁺	<i>RPM1</i> ⁻	<i>P</i>	<i>RPM1</i> ⁺	<i>RPM1</i> ⁻	<i>P</i>	<i>RPM1</i> ⁺	<i>RPM1</i> ⁻	<i>P</i>
T1	821.9 \pm 32.6	889.6 \pm 34.3	0.009	38.5 \pm 0.4	40.5 \pm 0.4	<0.001	1.23 \pm 0.05	1.48 \pm 0.05	<0.001
T3	670.3 \pm 28.0	729.1 \pm 28.3	0.008	38.2 \pm 0.4	39.5 \pm 0.4	0.151	1.21 \pm 0.04	1.36 \pm 0.05	0.001
T5	798.1 \pm 29.6	835.6 \pm 30.4	0.080	33.6 \pm 0.3	35.4 \pm 0.3	<0.001	0.94 \pm 0.03	1.03 \pm 0.04	0.003
T6	782.7 \pm 31.9	802.9 \pm 31.9	0.386	38.6 \pm 0.4	41.1 \pm 0.3	<0.001	1.31 \pm 0.05	1.42 \pm 0.05	0.015

Results are means \pm s.e.m.

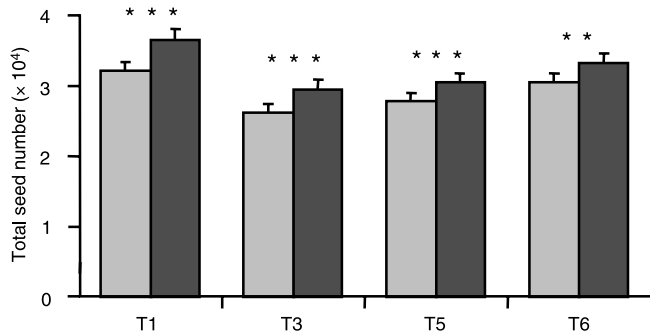


Figure 2 Total seed numbers. Seed production of *RPM1*⁺ sibs (light grey bars) and *RPM1*⁻ sibs (dark grey bars) in each transgenic line (T1, T3, T5, T6) is shown. Total seed number was estimated as the number of siliques multiplied by the average seed number per silique (*n* = 5). Results are means ± s.e.m. Data were analysed with paired *t*-tests for each background. Two asterisks, *P* < 0.01; three asterisks, *P* < 0.001.

functional) resistance alleles as susceptibility alleles. The issue of whether R-genes have a cost of resistance has been actively debated in the literature^{1,3,17–19}. This is the first definitive demonstration that such a cost exists. In addition, we find that the magnitude of this cost is surprisingly large, easily exceeding the 3.5% average fitness cost of disease resistance revealed by a meta-analysis of published studies of costs of resistance²⁰.

The cost of *RPM1* resistance is unlikely to be explained by the metabolic cost of *RPM1* synthesis, as the constitutive level of *RPM1* is extremely low¹⁰. Although we currently lack a molecular mechanism to explain the reduction in the fitness of resistant plants, two hypotheses can be proposed. First, *RPM1*⁺ plants might trigger the induction of plant defence pathways because of *RPM1* overexpression in the absence of pathogens. Although *RPM1* was expressed at normal levels in our greenhouse plants (and the salicylate-dependent defence pathway does not seem to have been induced), recent work on the rice-blast-resistance gene family demonstrates that R-gene expression levels can be markedly upregulated by environmental signals²¹. If this occurred during our field trial, then fitness could decline because R-gene overexpression can lead to constitutive defence response^{22,23}, cell death^{23–25} and even plant death²⁶. The second hypothesis is that basal levels of *RPM1* indirectly induce plant defence responses as a consequence of interactions with other R-proteins, the targets they guard, and the bacterial effectors (*Avr* proteins) they recognize^{15,27–29}. Distinguishing between these alternative hypotheses will be important for understanding R-gene structure/function and evolution.

With more than 100 R-gene loci spread across the *Arabidopsis* genome, many of which are likely to be segregating for resistance and susceptibility alleles, can the fitness cost of *RPM1* resistance be representative of other R-genes? We think not. First, the presence of so many loci segregating for alleles with 9% fitness costs would impose an impossibly large genetic load on populations. Second,

the fact that *RPM1* segregates for a long-lived polymorphism for resistance and susceptibility alleles could bias it towards having a large fitness cost of resistance. Theoretical models predict that resistance alleles with the largest costs are least likely to be driven to fixation in the species, and thus facilitate long-term maintenance of polymorphism³⁰. Our previous molecular evolutionary analyses of the *RPM1* flanking sequence suggested a trench warfare model in which resistance and susceptibility alleles fluctuate in response to pathogen epidemiology but are both maintained because of the costs and benefits of resistance³. The recent demonstration that pseudomonads attack *A. thaliana* in natural populations³¹ and the current demonstration of a substantial cost of resistance lend further support to this model. □

Methods

Cre-lox insertion of *RPM1*

To create *lox-RPM1-lox* lines, we cloned a 3.84-kb region from Columbia, containing *RPM1*, its minimal promoter and its full terminator, between two *lox* sites in the vector pBS246 (Gibco-BRL catalogue no. 10349-019; Life Technologies). There is relatively little non-coding DNA between *RPM1* and adjacent loci (577 base pairs (bp) 5' and 989 bp 3'), and our transgene contains almost all of this sequence. Thus, unless *RPM1 cis*-regulation extends into or across the adjacent loci, our transgene contains the entire *cis*-regulatory region. A 4-kb fragment with *lox* sequences on either side of *RPM1* was then cloned into the binary vector pBin19. This construct, which included the selectable marker nptII outside the *lox* sites, was introduced by means of vacuum infiltration into Bla-2.

To create *cre* lines, a 3.43-kb region containing *cre* with the 35S promoter and Nos3' terminator, as well as the selectable markers Basta and GUS, was cloned in the binary vector pCambia3301. This construct was used to create six *cre* lines of the susceptible ecotype Bla-2. The *lox-RPM1-lox* lines were emasculated and then pollinated by the *cre* lines. In the F₂ generation, the presence of *cre* was negatively selected with Basta (AgroEvo USA) diluted 1:1,100. The remaining plants were screened by PCR to identify an individual that had lost *RPM1* and its sib that had retained *RPM1*. After confirmation that these lines were not resistant to GUS or Basta, each pair was self-pollinated for five generations and the homozygosity of *RPM1*⁺ or *RPM1*⁻ was confirmed by PCR. Inserts were sequenced in each *RPM1*⁺ line to confirm their integrity, and in each *RPM1*⁻ line to confirm clean excision. Southern blots and anchor PCR tests were consistent with the presence of only a single insert for each transformed line.

Quantitative real-time PCR

Eight PCR replicates from three independent RNA extractions were run for each line on an ABI Prism 7700 sequence-detection system with TaqMan PCR core reagent (PE Biosystems). Leaves were sampled from 4-week-old plants. EF1a, an elongation factor, was used as an endogenous reference gene in the same reaction tube³².

Field experiment

Seedlings of each *RPM1*⁺ and *RPM1*⁻ line were germinated in plug trays containing Premier Pro-Mix in the University of Chicago greenhouse. At the four-leaf stage, 4,000 seedlings (500 per line) were transplanted into a field site in Downer's Grove, Illinois, in a pseudo-random design in which *RPM1*⁺ and *RPM1*⁻ sibs were paired, and lines were cycled throughout the field. Plants were set out in 20 rows of 200 each, spaced by 0.3 m within rows and by 1 m between rows. Plants were irrigated for 1 week to reduce transplantation shock, and then were sustained only by natural rainfall. Plants were hand-weeded once and received no protection from pests. Roughly 21% of plants died, but these were evenly distributed among the treatments. Pairs of plants were excluded from analysis if either individual died prematurely.

Field assay of bacteria

Ninety-six leaf samples (representing plants of all eight lines) were ground and plated on KB medium on two dates during the field experiment. Bacteria were found in 24 samples from day 14, and in 32 samples from day 30. Out of hundreds of colonies, 15 potentially distinct bacterial types were identified by general appearance (colour, size and growth pattern). Each type was tested for pathogenicity on tobacco at a concentration of 10⁸ colony-forming units per ml (ref. 33), sequenced for 16S rRNA (ref. 34) and compared to published sequences in GenBank. None of these bacterial isolates were pathogens, according to the tobacco HR test or their 16S identity. Finally, we used PCR to screen for the presence of *AvrRpm1* and *AvrB*. For *AvrRpm1*, we designed a pair of degenerate primers for conserved regions of the gene based on three homologous sequences in GenBank. We also screened with a pair of primers that reliably amplified the *P. syringae* gene. For *AvrB*, only a single published sequence was available. We screened with nine combinations of primer pairs based on the published sequence. We failed to detect the *AvrRpm1* or *AvrB* genes in any of our colonies.

Chemical analyses

Five replicates of each line were grown in the greenhouse and harvested at 3 weeks for chemical analysis. Leaf material was frozen in liquid nitrogen, freeze-dried and homogenized. Material for salicylic acid analysis was extracted three times with 70% methanol and quantified by high-performance liquid chromatography³⁵. Material for protein analysis was extracted in 0.25 ml of 0.05 M sodium phosphate buffer pH 7.0.

Table 3 Common haplotypes (more than two individuals) in *RIN4* gene among 96 *A. thaliana* accessions

Type	No. of accessions*	Amino acid location						Resistance genotype	
		38	56	89	129	134	147	<i>RPM1</i> ⁺	<i>RPM1</i> ⁻
1	41	-	-	-	-	-	-	30	11
2	17	V	-	-	T	A	-	14	3
3	14	-	P	-	T	A	-	12	2
4	11	-	-	D	-	-	-	10	1
5	5	-	-	-	T	A	-	4	1
	Consensus	M	H	G	S	T	V	70	18

*Eight accessions exhibited rare haplotypes.

Peroxidase activity was determined by following the oxidation of guaiacol for 1 min at 470 nm and was standardized by total protein content as previously described³⁶.

Bioassay with *P. syringae* pv. *tomato* DC3000

Fifteen replicates of each line were challenged by infiltration of three leaves with 10⁴ colony-forming units per ml ($D_{600} = 0.002$) after 3 weeks of plant growth. After 5 days, leaf discs were removed, ground and plated on KB medium to determine the concentration of bacteria.

Received 18 February; accepted 18 March 2003; doi:10.1038/nature01588.

1. Grant, M. R. *et al.* Independent deletions of a pathogen-resistance gene in *Brassica* and *Arabidopsis*. *Proc. Natl Acad. Sci. USA* **87**, 15843–15848 (1998).
2. Caicedo, A. L., Schaal, B. A. & Kunkel, B. N. Diversity and molecular evolution of the *RPS2* resistance gene in *Arabidopsis thaliana*. *Proc. Natl Acad. Sci. USA* **96**, 302–306 (1999).
3. Stahl, E. A., Dwyer, G., Mauricio, R., Kreitman, M. & Bergelson, J. Dynamics of disease resistance polymorphism at the *Rpm1* locus of *Arabidopsis*. *Nature* **400**, 667–671 (1999).
4. Tian, D., Araki, H., Stahl, E., Bergelson, J. & Kreitman, M. Signature of balancing selection in *Arabidopsis*. *Proc. Natl Acad. Sci. USA* **99**, 11525–11530 (2002).
5. Mauricio, R., Korves, T., Stahl, E. A., Kreitman, M. & Bergelson, J. Natural selection for polymorphism in the disease resistance gene *RPS2* of *Arabidopsis*. *Genetics* **163**, 735–746 (2003).
6. Simms, E. L. & Rausher, M. D. Costs and benefits of plant resistance to herbivory. *Am. Nat.* **130**, 570–581 (1987).
7. Bergelson, J., Dwyer, G. & Emerson, J. J. Models and data on plant–enemy coevolution. *Annu. Rev. Genet.* **35**, 469–499 (2001).
8. Boyes, D. C., Nam, J. & Dangel, J. L. The *Arabidopsis thaliana* *RPM1* disease resistance gene product is a peripheral plasma membrane protein that is degraded coincident with the hypersensitive response. *Proc. Natl Acad. Sci. USA* **95**, 15849–15854 (1998).
9. Bisgrove, S. R., Simonich, M. T., Smith, N. M., Sattler, A. & Innes, R. W. A disease resistance gene in *Arabidopsis* with specificity for two different pathogen avirulence genes. *Plant Cell* **6**, 927–933 (1994).
10. Grant, M. R. *et al.* Structure of the *Arabidopsis* *RPM1* gene enabling dual specificity disease resistance. *Science* **269**, 843–846 (1995).
11. Redei, G. *P. Arabidopsis* as a genetic tool. *Annu. Rev. Genet.* **9**, 111–127 (1986).
12. Ow, D. W. & Medberry, S. L. Genome manipulation through site-specific recombination. *Crit. Rev. Plant Sci.* **14**, 239–261 (1995).
13. Howe, C. *Gene Cloning and Manipulation* (Cambridge Univ. Press, Cambridge, 1995).
14. Whalen, M. C., Innes, R. W., Bent, A. F. & Staskawicz, B. J. Identification of *Pseudomonas syringae* pathogens of *Arabidopsis* and a bacterial locus determining avirulence on both *Arabidopsis* and soybean. *Plant Cell* **3**, 49–59 (1991).
15. Mackey, D., Holt, B. E., Wiig, A. & Dangel, J. L. RIN4 interacts with *Pseudomonas syringae* Type III effector molecules and is required for RPM1-mediated resistance in *Arabidopsis*. *Cell* **108**, 743–754 (2002).
16. Jørgensen, J. H. & Jensen, H. P. Effect of ‘unnecessary’ powdery mildew resistance genes on agronomic properties of spring barley. *Norsk Landbruksforskning, Suppl.* **9**, 125–130 (1990).
17. Brown, J. K. M. Yield penalties of disease resistance in crops. *Curr. Opin. Plant Biol.* **5**, 1–6 (2002).
18. Rausher, M. D. Co-evolution and plant resistance to natural enemies. *Nature* **411**, 857–864 (2001).
19. Stuiver, M. H. & Custers, J. H. H. V. Engineering disease resistance in plants. *Nature* **411**, 865–868 (2001).
20. Bergelson, J. & Purrington, C. B. Surveying patterns in the cost of resistance in plants. *Am. Nat.* **148**, 536–558 (1996).
21. Wang, Z.-W., Yamanouchi, U., Katayose, Y., Sasaki, T. & Yano, M. Expression of the *Pib* rice-blast-resistance gene family is up-regulated by environmental conditions favouring infection and by chemical signals that trigger secondary plant defences. *Plant Mol. Biol.* **47**, 653–661 (2001).
22. Oldroyd, G. E. D. & Staskawicz, B. J. Genetically engineered broad-spectrum disease resistance in tomato. *Proc. Natl Acad. Sci. USA* **95**, 10300–10305 (1998).
23. Tang, X. *et al.* Overexpression of *Pto* activates defense responses and confers broad resistance. *Plant Cell* **11**, 15–29 (1999).
24. Mindrinos, M., Katagiri, F., Yu, G. & Ausubel, F. M. The *A. thaliana* disease resistance gene *RPS2* encodes a protein containing a nucleotide-binding site and leucine-rich repeats. *Cell* **78**, 1089–1099 (1994).
25. Tao, Y., Yuan, F., Leister, R. T., Ausubel, F. M. & Katagiri, F. Mutational analysis of the *Arabidopsis* nucleotide binding site-leucine-rich repeat resistance gene *RPS2*. *Plant Cell* **12**, 2541–2554 (2000).
26. Holt, B. J. *et al.* An evolutionarily conserved mediator of plant disease resistance gene function is required for normal *Arabidopsis* development. *Dev. Cell* **2**, 807–817 (2002).
27. van der Biezen, E. A. & Jones, J. D. G. Plant disease resistance proteins and the gene for gene concept. *Trends Biochem. Sci.* **23**, 454–456 (1998).
28. Dangel, J. L. & Jones, J. D. G. Plant pathogens and integrated defence responses to infection. *Nature* **411**, 826–832 (2001).
29. Mackey, D., Belkadir, Y., Alonso, J. M., Ecker, J. R. & Dangel, J. L. *Arabidopsis* RIN4 is a target of the Type III virulence effector *AvrRpt2* and modulates RPS2-mediated resistance. *Cell* **112**, 379–389 (2003).
30. Gillespie, J. H. Natural selection for resistance to epidemics. *Ecology* **56**, 493–495 (1975).
31. Jakob, K. *et al.* *Pseudomonas viridiflava* and *P. syringae*—natural pathogens of *Arabidopsis thaliana*. *Mol. Plant–Microbe Interact.* **15**, 1195–1203 (2002).
32. Heid, C. A., Stevens, J., Livak, K. J. & Williams, P. M. Real time quantitative PCR. *Genome Res.* **6**, 986–994 (1996).
33. Klement, Z. Rapid detection of the pathogenicity of phytopathogenic *Pseudomonads*. *Nature* **199**, 299–300 (1963).
34. Moore, E. R. B. *et al.* The determination and comparison of the 16S rRNA gene sequences of species of the genus *Pseudomonas* (sensu stricto) and estimation of the natural intragenetic relationships. *Syst. Appl. Microbiol.* **19**, 478–492 (1996).
35. Dewdney, J. *et al.* Three unique mutants of *Arabidopsis* identify *eds* loci required for limiting growth of a biotrophic fungal pathogen. *Plant J.* **24**, 205–218 (2000).
36. Traw, M. B., Kim, J., Enright, S., Cipollini, D. F. & Bergelson, J. Negative cross-talk between the salicylate and jasmonate-mediated pathways in the Wassilewskija ecotype of *Arabidopsis thaliana*. *Mol. Ecol.* **12**, 1125–1135 (2003).

Acknowledgements We thank J. Dangel for feedback, and members of the Department of Ecology and Evolution for assistance in the field. This research was supported by NIH grants to J.B.

Competing interests statement The authors declare that they have no competing financial interests.

Correspondence and requests for materials should be addressed to J.B. (jbergels@midway.uchicago.edu).

.....

Non-classical receptive field mediates switch in a sensory neuron’s frequency tuning

Maurice J. Chacron*†, Brent Doiron*†, Leonard Maler†, André Longtin* & Joseph Bastian‡

* Physics Department, University of Ottawa, Ottawa, Ontario, Canada K1N 6N5
 † Department of Cellular and Molecular Medicine, University of Ottawa, Ottawa, Ontario, Canada K1H 8M5
 ‡ Department of Zoology, University of Oklahoma, Norman, Oklahoma 73019, USA

Animals have developed stereotyped communication calls to which specific sensory neurons are well tuned^{1,2}. These communication calls must be discriminated from environmental signals such as those produced by prey. Sensory systems might have evolved neural circuitry to encode both categories. In weakly electric fish, prey and communication signals differ in their spatial extent and frequency content^{3,4}. Here we show that stimuli of different spatial extents mimicking prey and communication signals cause a switch in the frequency tuning and spike-timing precision of electrosensory pyramidal neurons, resulting in the selective and optimal encoding of both stimulus categories. As in other sensory systems⁵, pyramidal neurons respond only to stimuli located within a restricted region of space known as the classical receptive field (CRF)⁶. In some systems, stimulation outside the CRF but within a non-classical receptive field (nCRF) can modulate the neural response to CRF stimulation even though nCRF stimulation alone fails to elicit responses^{7,8}. We show that pyramidal neurons possess a nCRF and that it can modulate the response to CRF stimuli to induce this neurobiological switch in frequency tuning.

The complex statistical structure of many naturalistic visual⁹ and auditory¹⁰ stimuli makes our interpretation of neural responses to these stimuli difficult and often prevents clearcut correlations of the responses with behaviour. Weakly electric fish offer a simple system for studying the differential encoding of natural stimuli because there is a clear spatiotemporal distinction between prey and communication stimuli. Amplitude modulations (AMs) of the electric fish’s self-generated electric organ discharge (EOD) contain information relevant to both types of stimulus¹¹. Epidermal electroreceptors encode these AMs precisely¹² and provide synaptic input¹³ to pyramidal neurons of the electrosensory lateral line lobe (ELL), whose antagonistic centre-surround CRF structure⁶ resembles that of visual neurons⁵. Relative motion of the fish near prey during feeding produces low-frequency (less than 10 Hz) spatially localized AMs³. However, communication signals from conspecifics produce high-frequency (more than 50 Hz) spatially diffuse AMs⁴.

To provide naturalistic stimuli that mimic prey and communication signals, we used two stimulation geometries (see Methods). Local stimulus geometry provides AMs whose spatial extent is similar to that produced by prey, while global stimulus geometry produces spatially diffuse AMs similar to communication signals

